Magnetic Fields and Polarization in Blazar jets: progress since 2013

Jets 2016, Malaga, Espana

1. **Magnetically arrested disks (MADs)**
2. **Evidence for strong magnetic fields near SMBHs**
3. **Polarized Maximum Entropy imaging**
4. **What the EHT might see**
5. **Al Marscher**

1. **Magnetically arrested disks (MADs)**

2. **Evidence for strong magnetic fields near SMBHs**
   Kazu Akiyama, Jose Louis Gomez, Michael Johnson ++

3. **Polarized Maximum Entropy imaging**
   Vincent Fish

4. **What the EHT might see**
   Dimitrios Psaltis++

5. **Al Marscher**

Measured magnetic flux of the jet, Φ_{jet}, versus $L_{acc}^{1/2} M$.

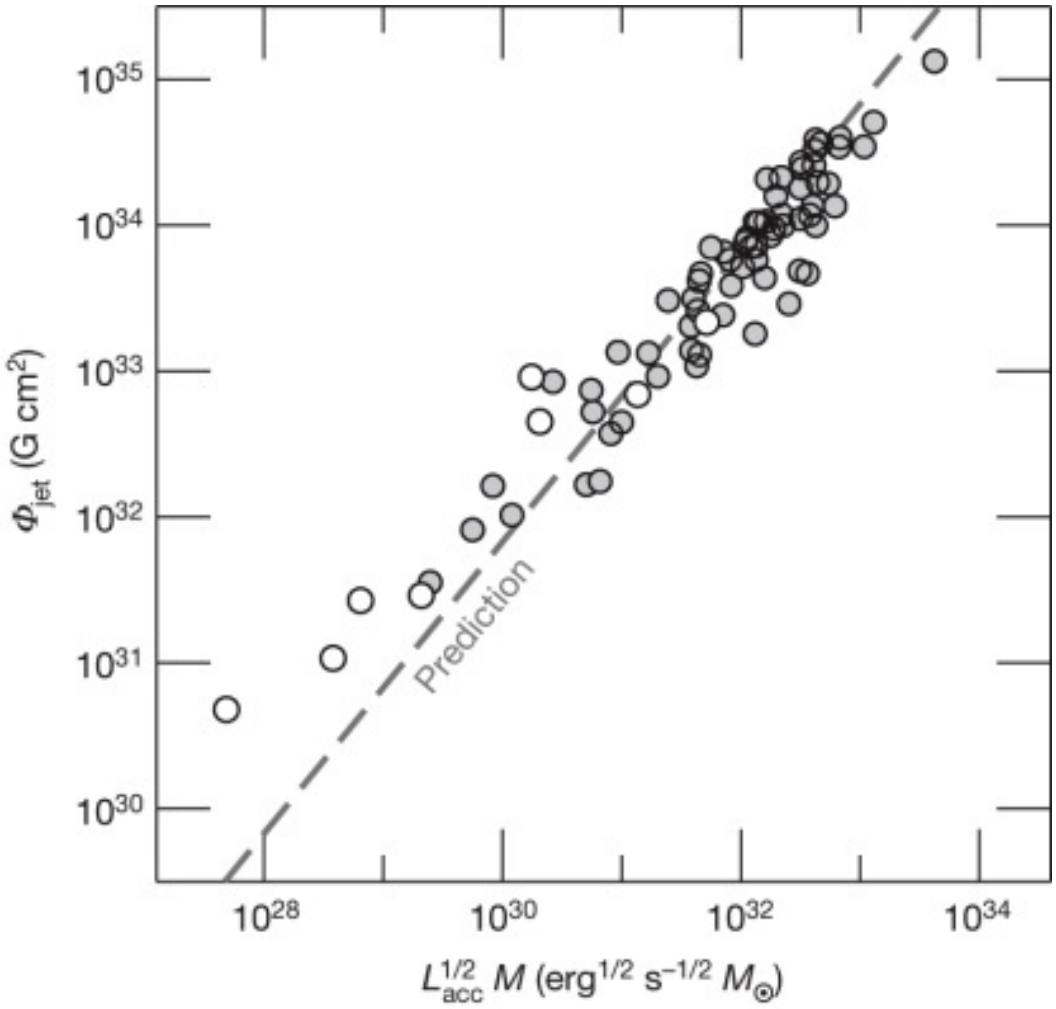

M Zamaninasab *et al. Nature* **510**, 126-128 (2014) doi:10.1038/nature13399

Predicted magnetic flux:

$$\Phi_{\rm jet} \approx 50 \left(\dot{M} r_{\rm g}^2 c \right)^{1/2}$$ to arrest accretion

$$50 \left(\dot{M} r_{\rm g}^2 c \right)^{1/2} = 2.4 \times 10^{34} \left[\frac{\eta}{0.4} \right]^{-1/2} \left[\frac{M}{10^9 M_\odot} \right] \left[\frac{L_{\rm acc}}{1.26 \times 10^{47} {\rm erg\ s^{-1}}} \right]^{1/2} {\rm G\ cm^2}$$

"Observed" magnetic flux:

$$\Phi_{\rm jet} = 1.2 \times 10^{34} f(a_*) \Gamma \theta_{\rm j} \left[\frac{M}{10^9 M_\odot} \right] \left[\frac{B'_{\rm 1pc}}{1 {\rm G}} \right]$$

$B'_{\rm 1pc}$ is derived from the measured core shift

Measured magnetic flux of the jet, Φ_{jet}, versus $L_{acc}^{1/2} M$.

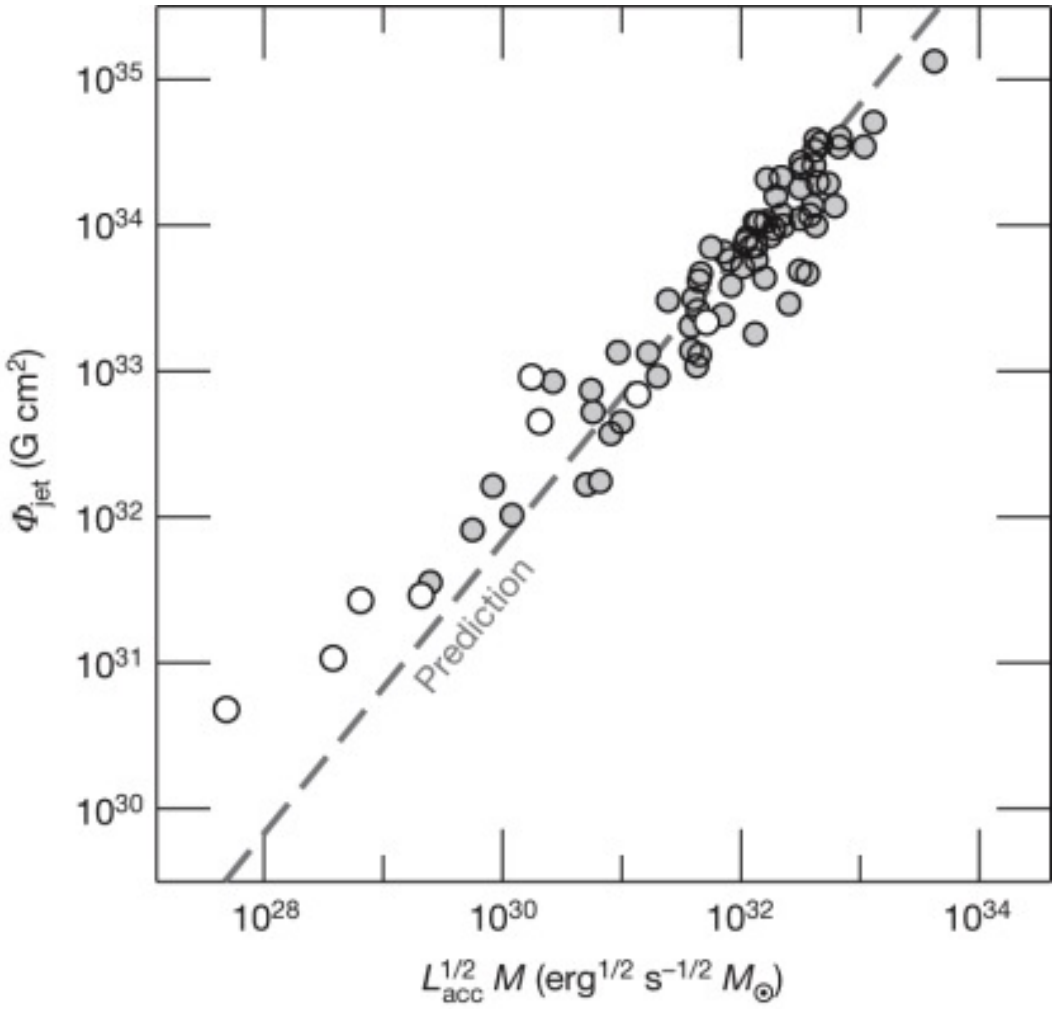

M Zamaninasab *et al. Nature* **510**, 126-128 (2014) doi:10.1038/nature13399

2. Evidence for strong magnetic fields near SMBHs

(a) large Rotation Measures in unresolved sources

(b) GMVA and EHT observations

Marrone ++ (2006): multiple observations of Sgr A* with the SMA at 230 and 350 GHz.

Mean ten epoch Rotation Measure is $(-5.6 \pm 0.7) \times 10^5$ rad m^{-2}

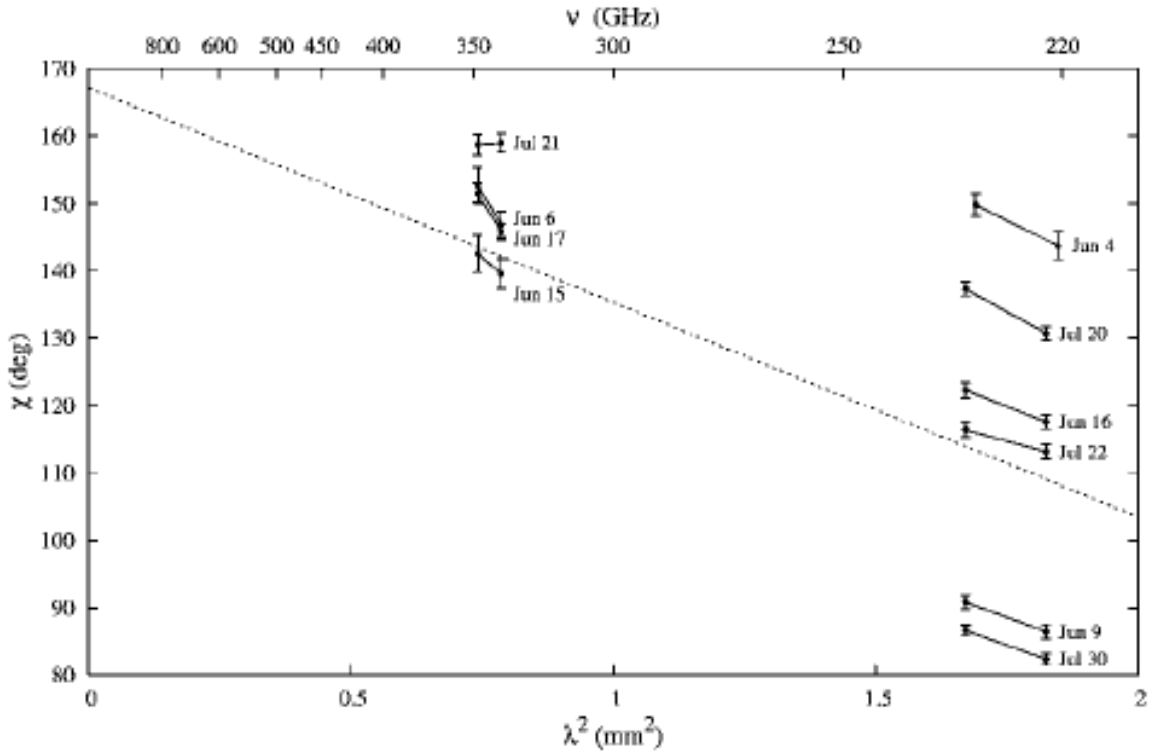

Marrone ++ (2006): multiple observations of Sgr A* with the SMA at 230 and 350 GHz.

Mean ten epoch Rotation Measure is $(-5.6 \pm 0.7) \times 10^5$ rad m^{-2}

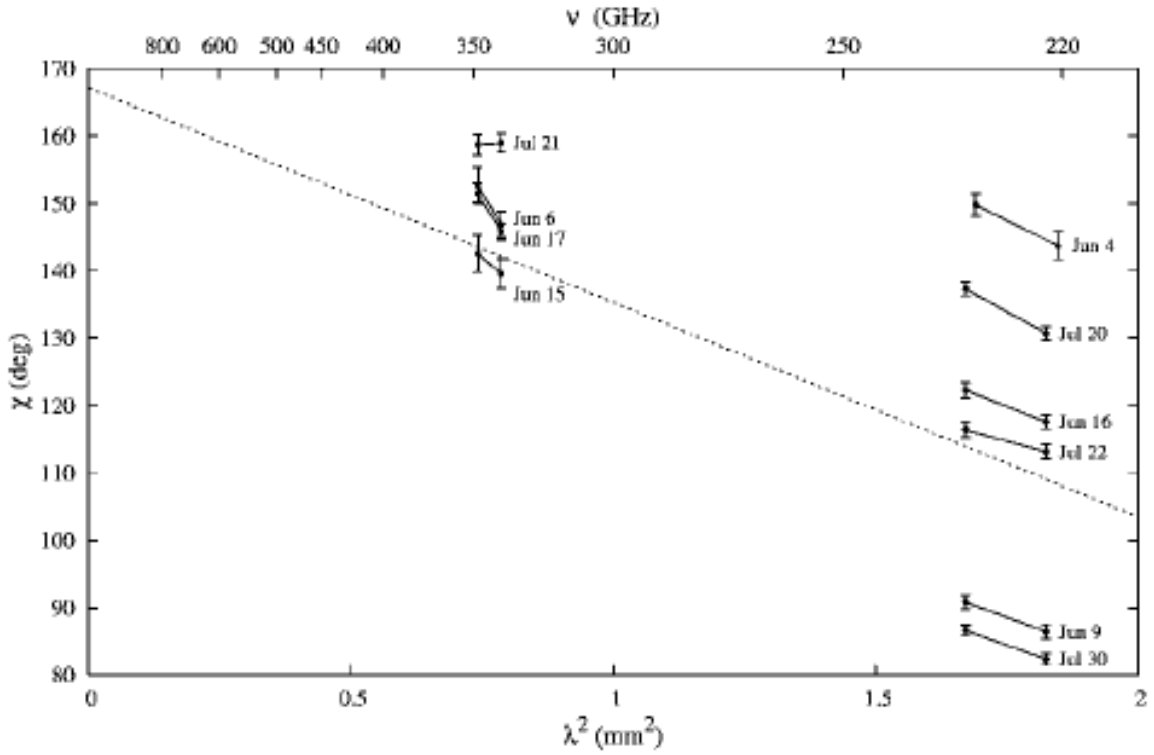

$$\frac{\mathrm{RM}}{[\mathrm{rad\ m^{-2}}]} = 0.81 \int_{\mathrm{source}}^{\mathrm{observer}} \frac{n_e}{[\mathrm{cm^{-3}}]} \frac{B_{\|}}{[\mu\mathrm{G}]} \frac{\mathrm{d}l}{[\mathrm{pc}]},$$

Marrone ++ (2006): multiple observations of Sgr A* with the SMA at 230 and 350 GHz.

Mean ten epoch Rotation Measure is $(-5.6 \pm 0.7) \times 10^5$ rad m^{-2}

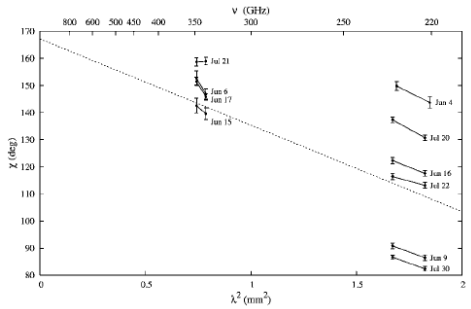

$$\frac{\mathrm{RM}}{[\mathrm{rad\ m^{-2}}]} = 0.81 \int_{\mathrm{source}}^{\mathrm{observer}} \frac{n_e}{[\mathrm{cm^{-3}}]} \frac{B_{||}}{[\mu\mathrm{G}]} \frac{\mathrm{d}l}{[\mathrm{pc}]},$$

To think about: (a) how to disentangle n_e and $B_{||}$

(b) how to estimate magnetic field reversals

Marrone ++ (2006): multiple observations of Sgr A* with the SMA at 230 and 350 GHz.

Mean ten epoch Rotation Measure is $(-5.6 \pm 0.7) \times 10^5$ rad m^{-2}

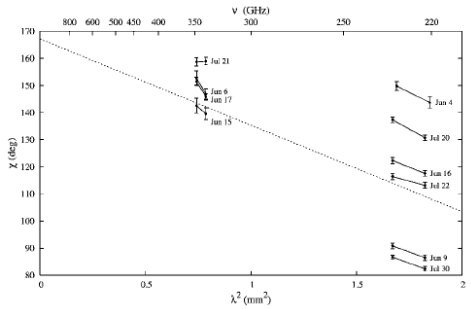

$$\frac{\mathrm{RM}}{[\mathrm{rad\ m^{-2}}]} = 0.81 \int_{\mathrm{source}}^{\mathrm{observer}} \frac{n_e}{[\mathrm{cm^{-3}}]} \frac{B_{||}}{[\mu\mathrm{G}]} \frac{\mathrm{d}l}{[\mathrm{pc}]},$$

To think about: (a) how to disentangle n_e and $B_{||}$

(b) how to estimate magnetic field reversals

But

(a) with plausible assumptions, Rotation Measures have been used to constrain accretion rates

(b) n_e and $B_{||}$ are both *direct* products of the GRMHD simulations (relativistic electrons are not, they are added post hoc), so a good RM image may be one of the best tests of the GRMHD simulations themselves.

Fig. 1 ALMA image of the gravitationally lensed AGN PKS 1830−211 at 250 GHz, taken on 30 June 2014.

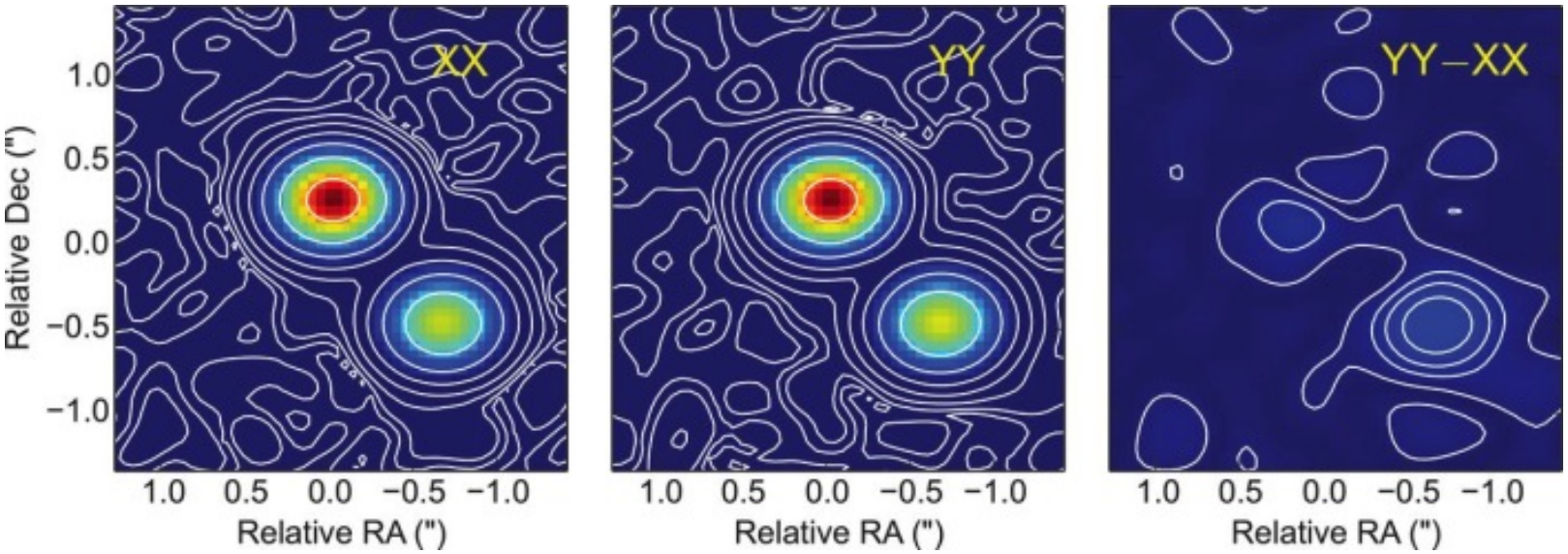

Ivan Martí-Vidal et al. Science 2015;348:311-314

Fig. 1 ALMA image of the gravitationally lensed AGN PKS 1830−211 at 250 GHz, taken on 30 June 2014.

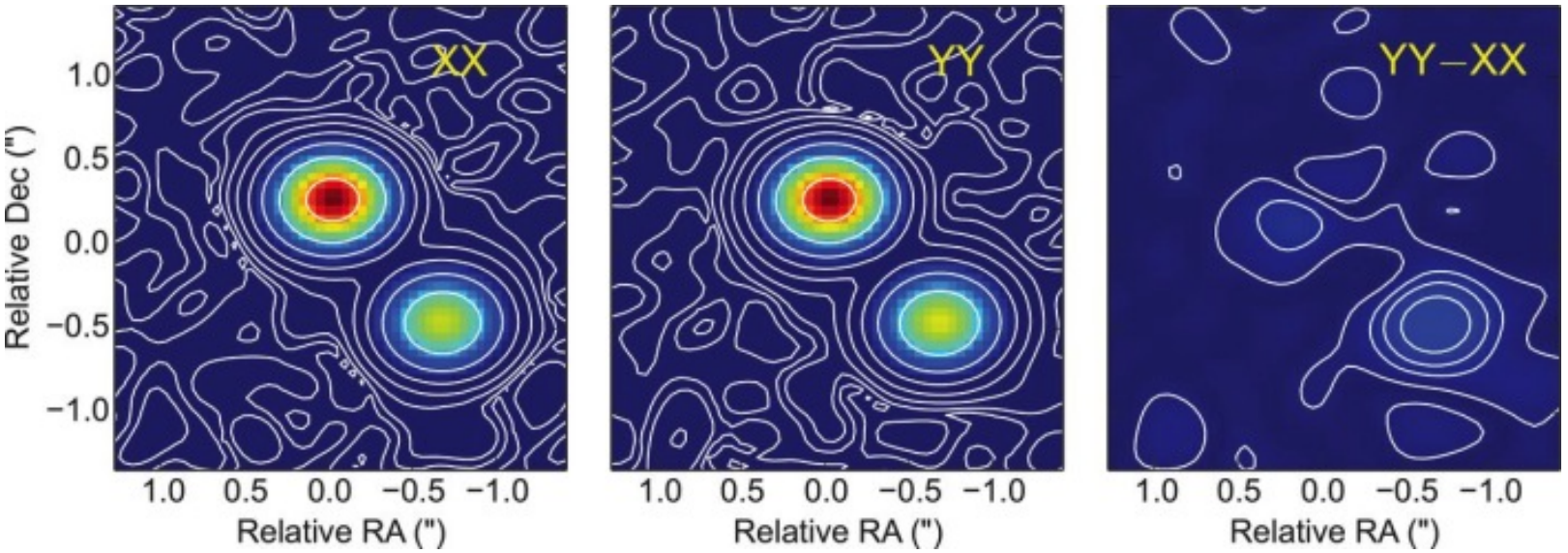

$$R_{pol} = \frac{1}{2}\left(\frac{R^{ij}_{XX}}{R^{ij}_{YY}} - 1\right)$$

Ivan Martí-Vidal et al. Science 2015;348:311-314

Fig. 4 Fits of our three epochs with quasi-simultaneous observations at 250 and 300 GHz to the model given in Eq. 1.

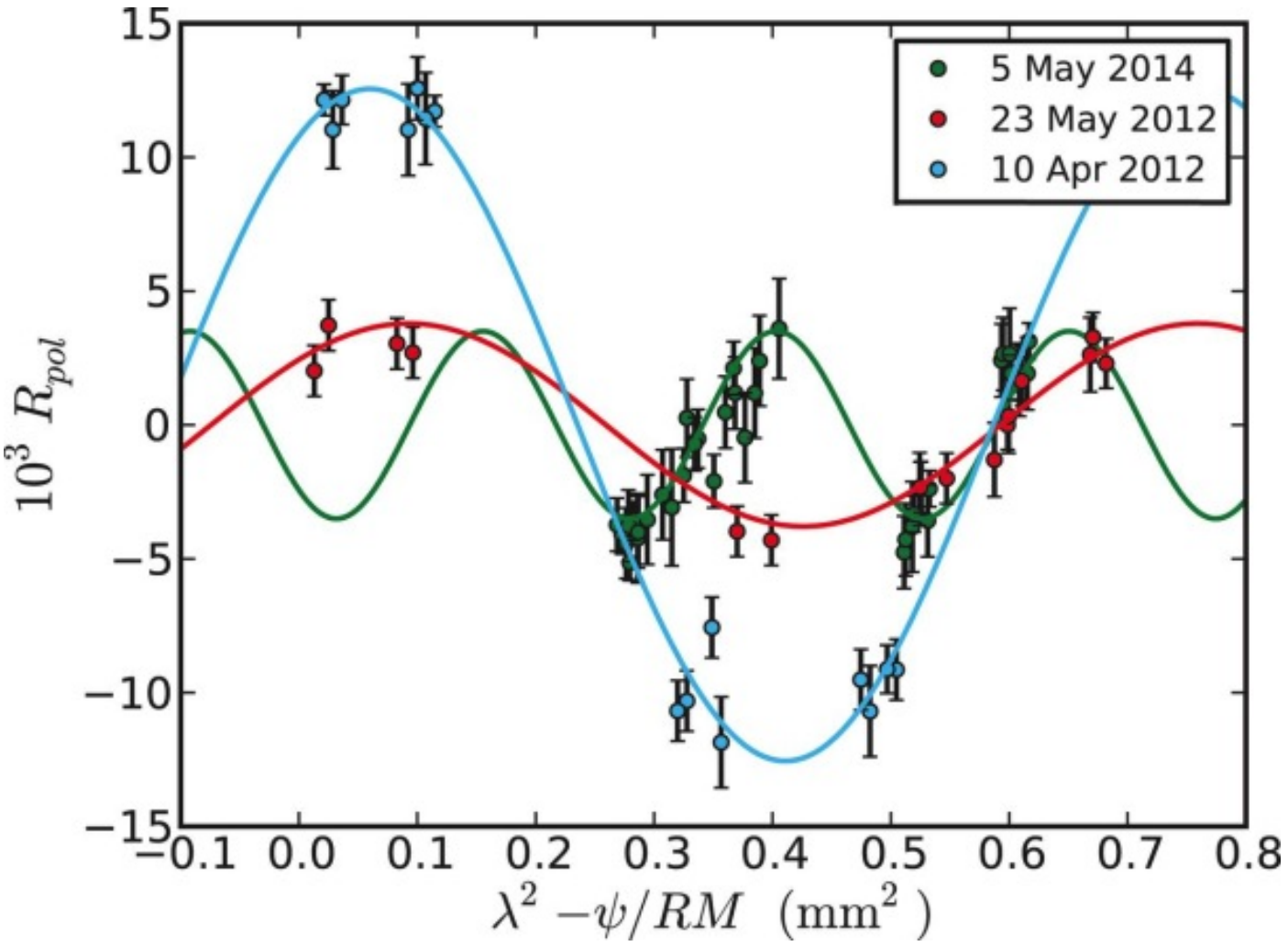

Published by AAAS

Fig. 4 Fits of our three epochs with quasi-simultaneous observations at 250 and 300 GHz to the model given in Eq. 1.

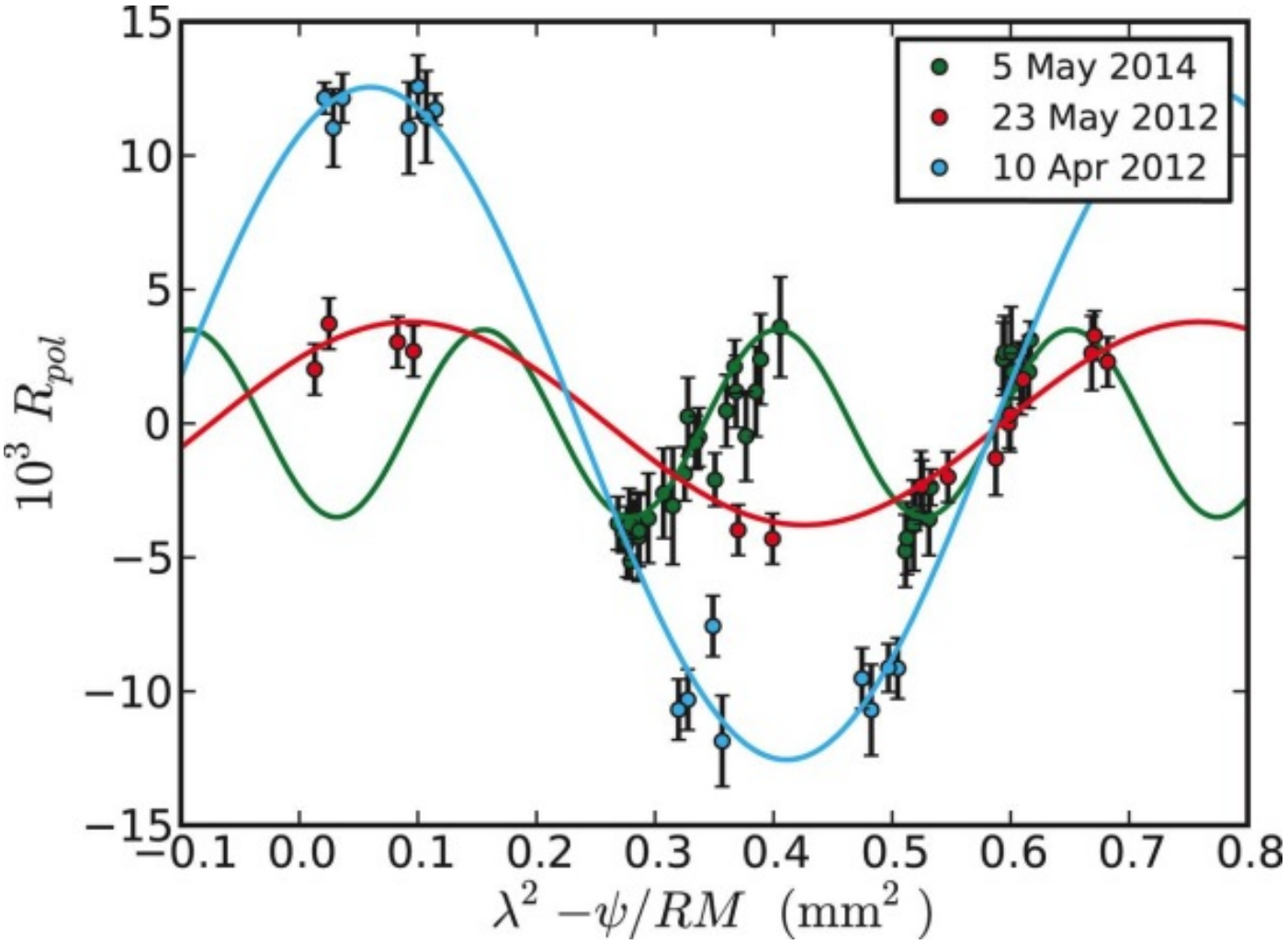

Rest frame Rotation Measure is in range (1 – 3) x 10^8 rad m^{-2}

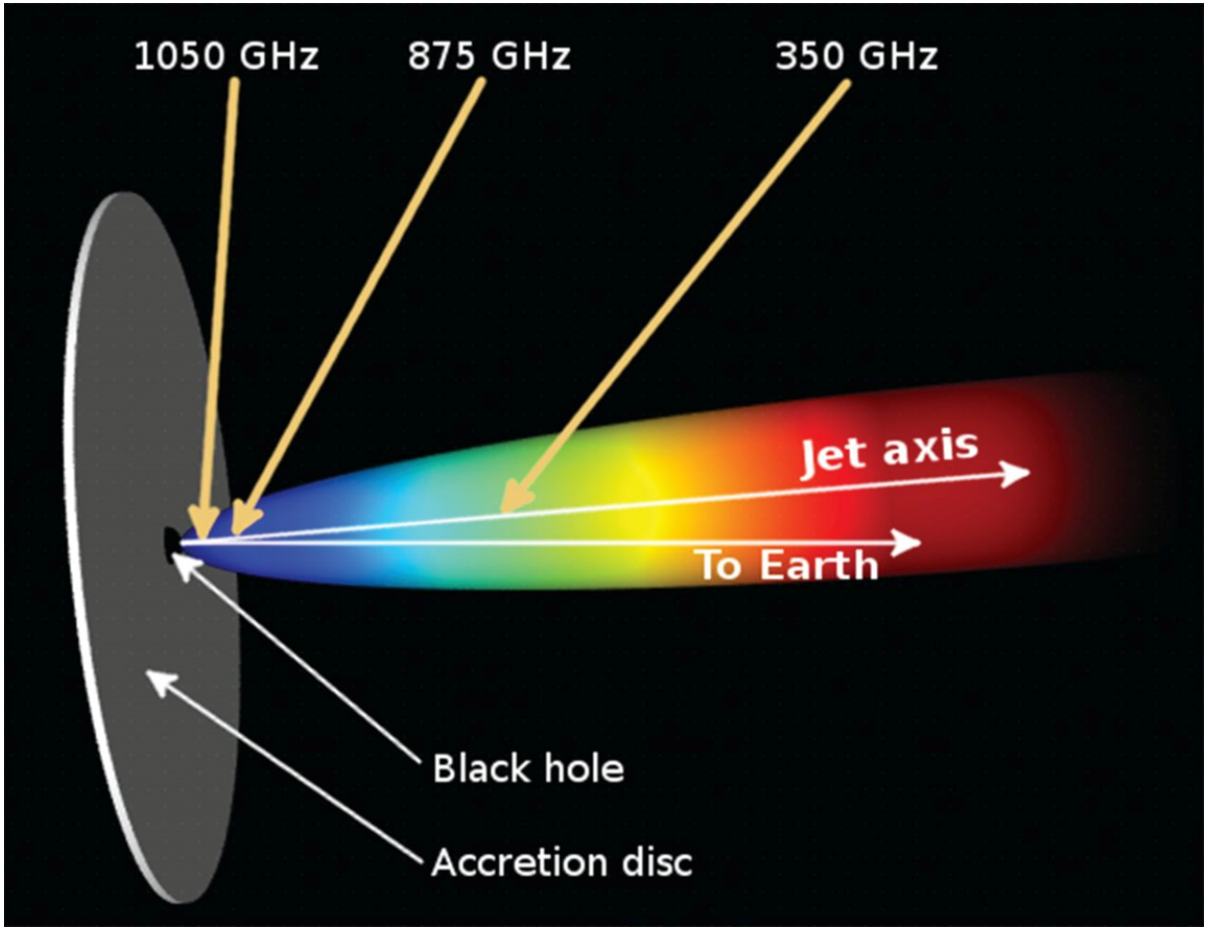
1050 GHz
875 GHz
350 GHz
Jet axis
To Earth
Black hole
Accretion disc

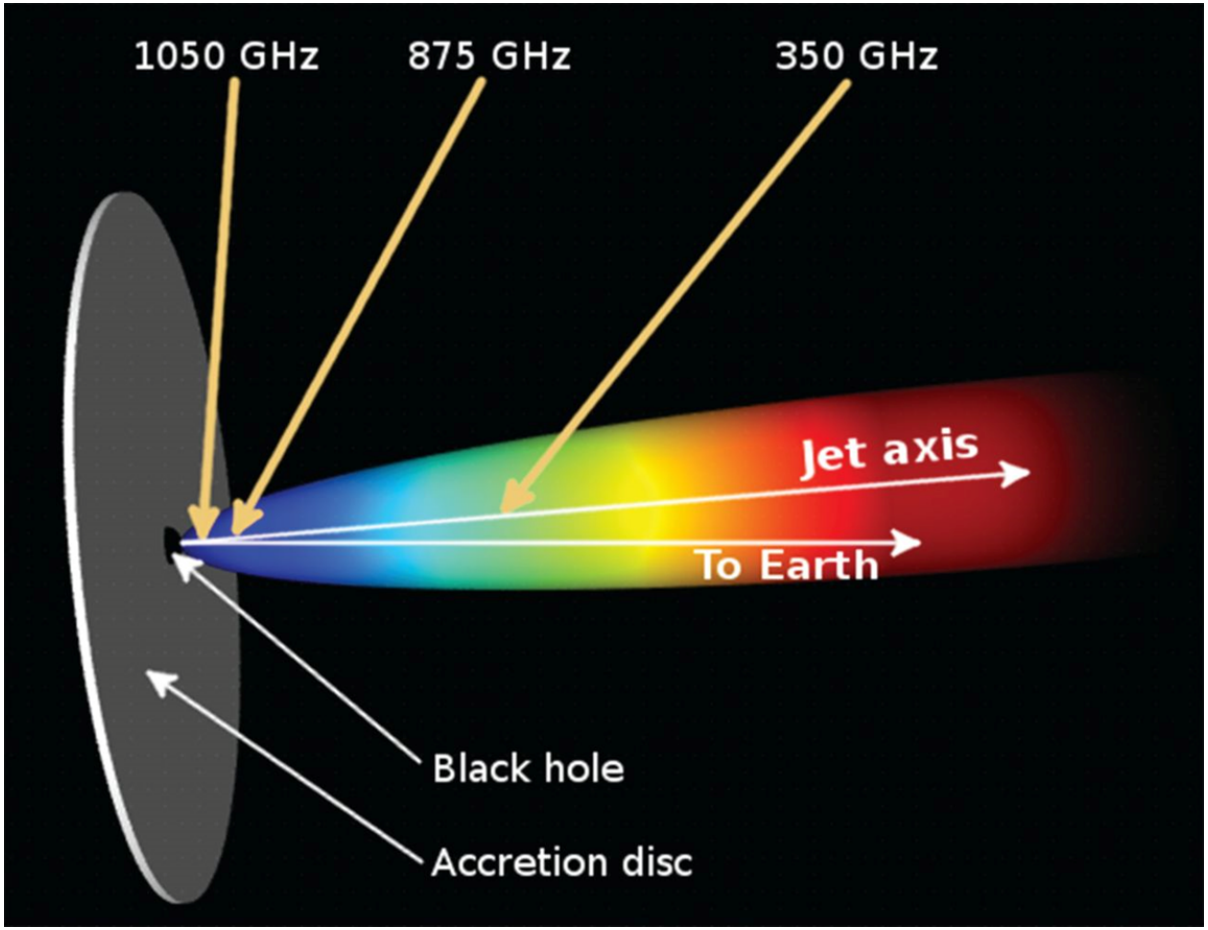

This means rotation measure is probably a function of wavelength and you do not expect the EVPA to vary as λ^2. (In the Blandford-Königl (1979) model, the (internal) RM ~ λ^{-2}, so the EVPA ~ λ^0!)

2. Evidence for strong magnetic fields near SMBHs

(a) large Rotation Measures in unresolved sources

(b) GMVA and EHT observations

BL Lac Gómez ++ (2016) GMVA + RadioAstron

u-v coverage at 22 GHz

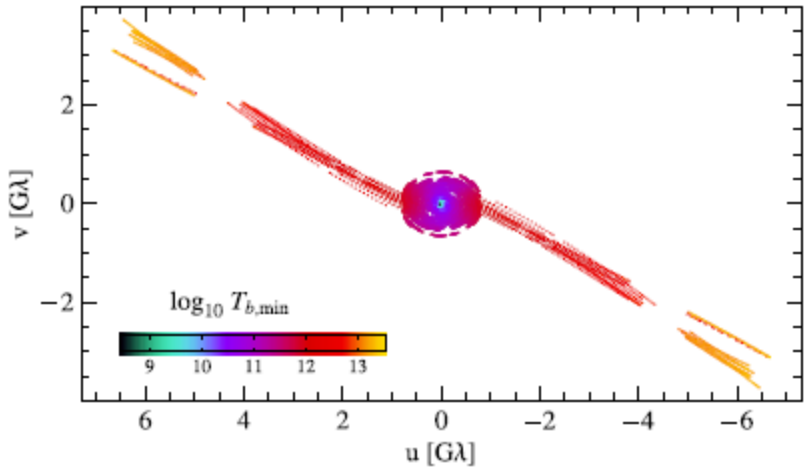

Rotation Measure Map constructed from images at 15, 22 and 43 GHz

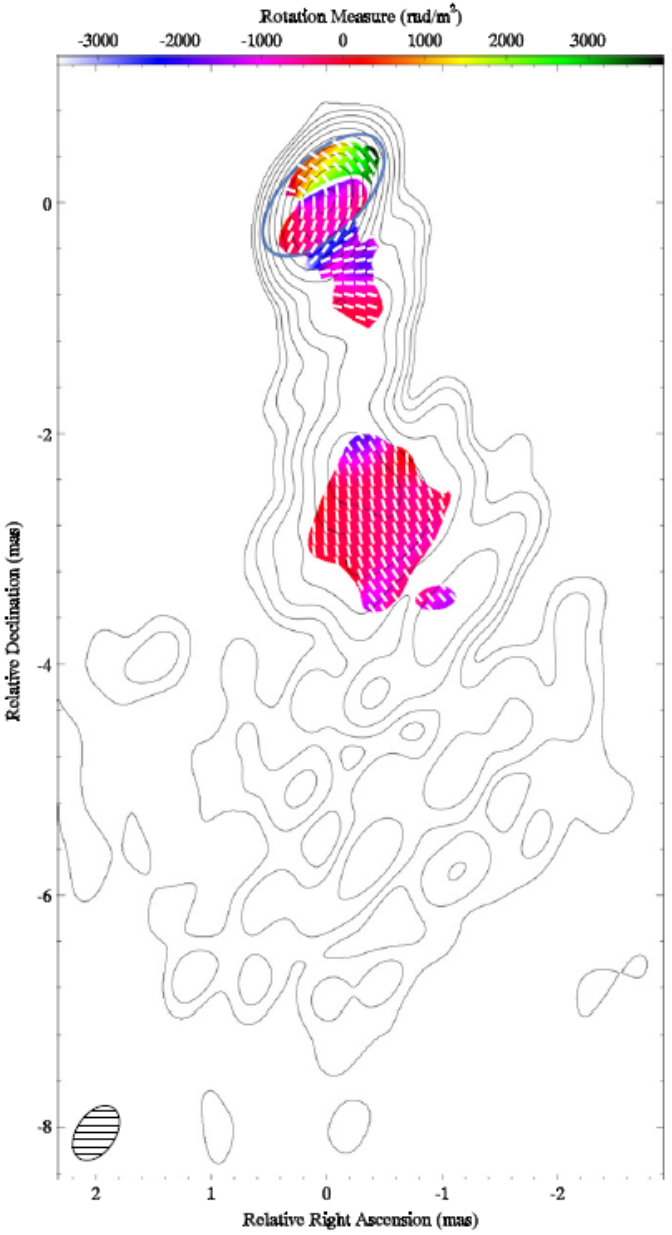

M87 Hada ++ (2016) VLBA + GBT 86 GHz

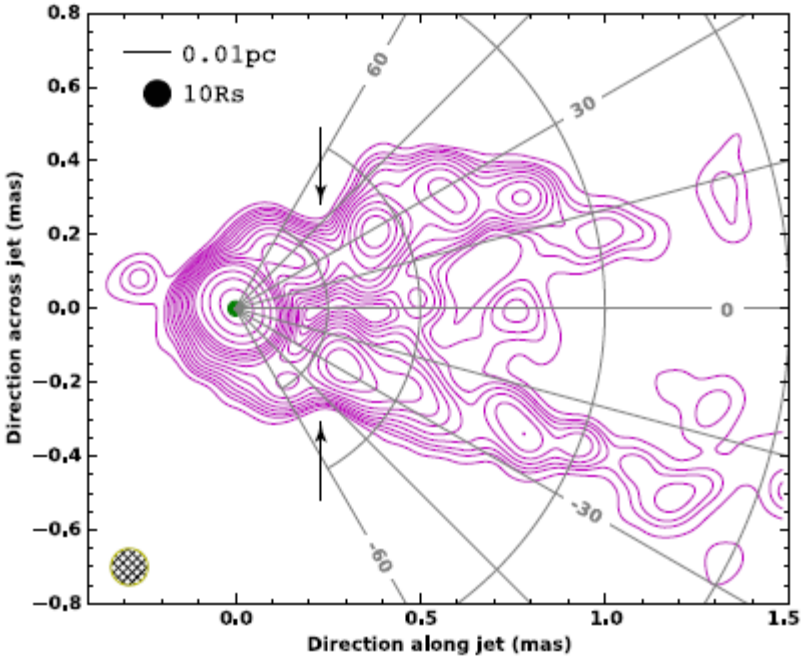

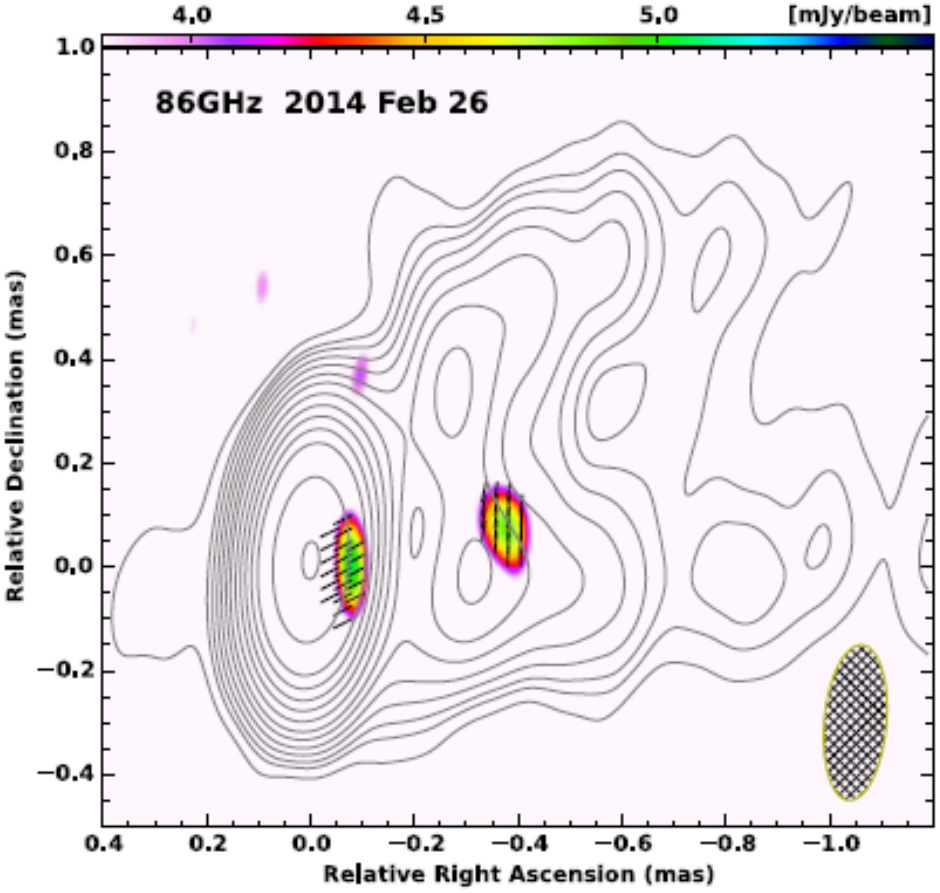

3C 273 Hada ++ (2016) VLBA + GBT 86 GHz, VLBA 43 GHz

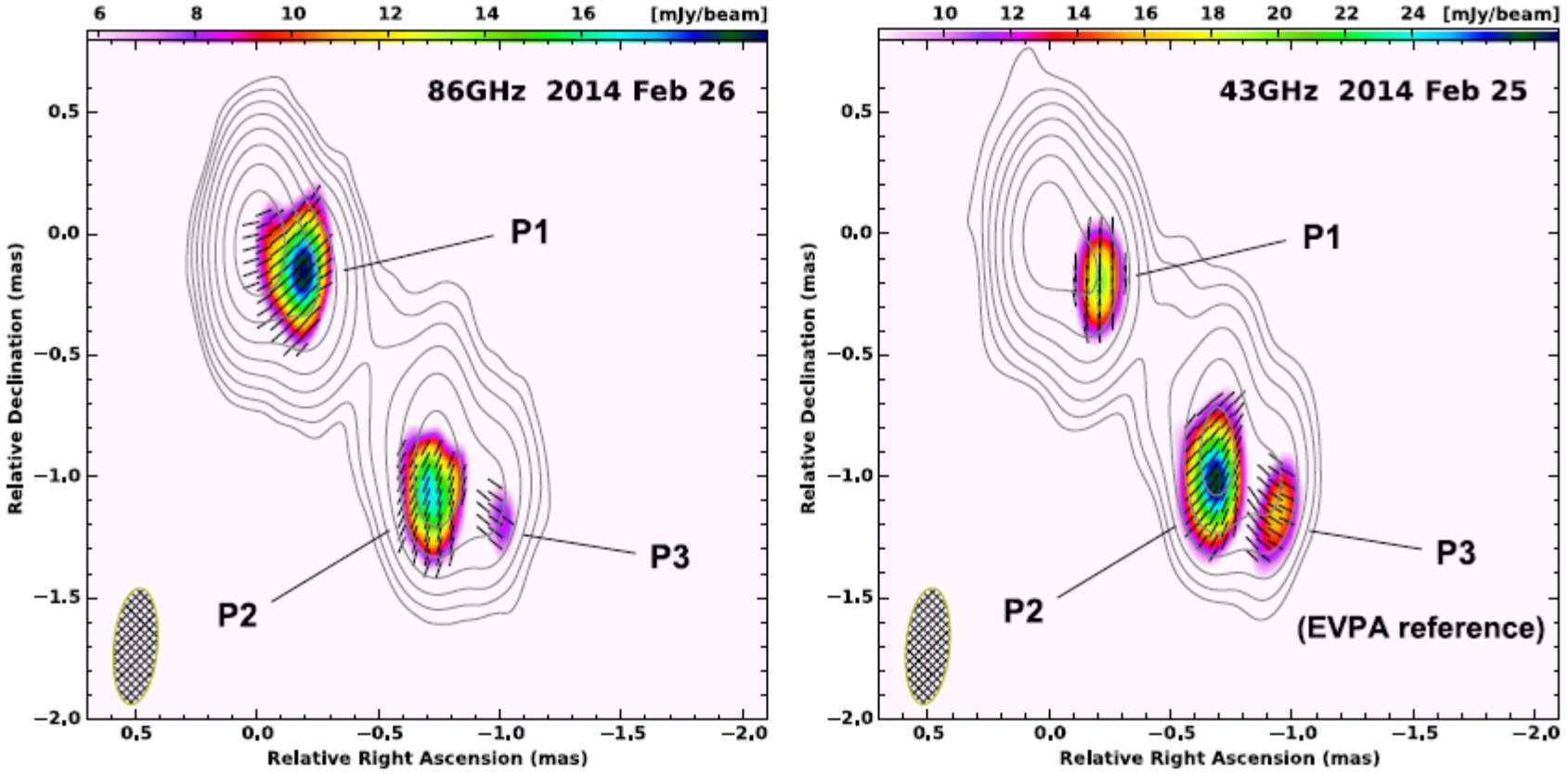

RM difference between P1 and P3 is > 2.4 x 10^4 rad m^{-2} (cf. Attridge ++ 2005)

Resolved magnetic-field structure and variability near the event horizon of Sagittarius A*

Michael D. Johnson[1,*], Vincent L. Fish[2], Sheperd S. Doeleman[1,2], Daniel P. Marrone[3], Richard L. Plambeck[4], John F. C. Wardle[5], Kazunori Akiyama[2,6,7], Keiichi Asada[8], Christopher Beaudoin[2], Lindy

+ 31 co-authors.

Science, Volume 350, Issue 6265, pp. 1242-1245 (2015)

Resolved magnetic-field structure and variability near the event horizon of Sagittarius A*

Michael D. Johnson[1,*], Vincent L. Fish[2], Sheperd S. Doeleman[1,2], Daniel P. Marrone[3], Richard L. Plambeck[4], John F. C. Wardle[5], Kazunori Akiyama[2,6,7], Keiichi Asada[8], Christopher Beaudoin[2], Lindy

+ 31 co-authors.

Science, Volume 350, Issue 6265, pp. 1242-1245 (2015)

+ 39 pages of Supplementary Material

BL Lac: a slightly resolved calibrator source

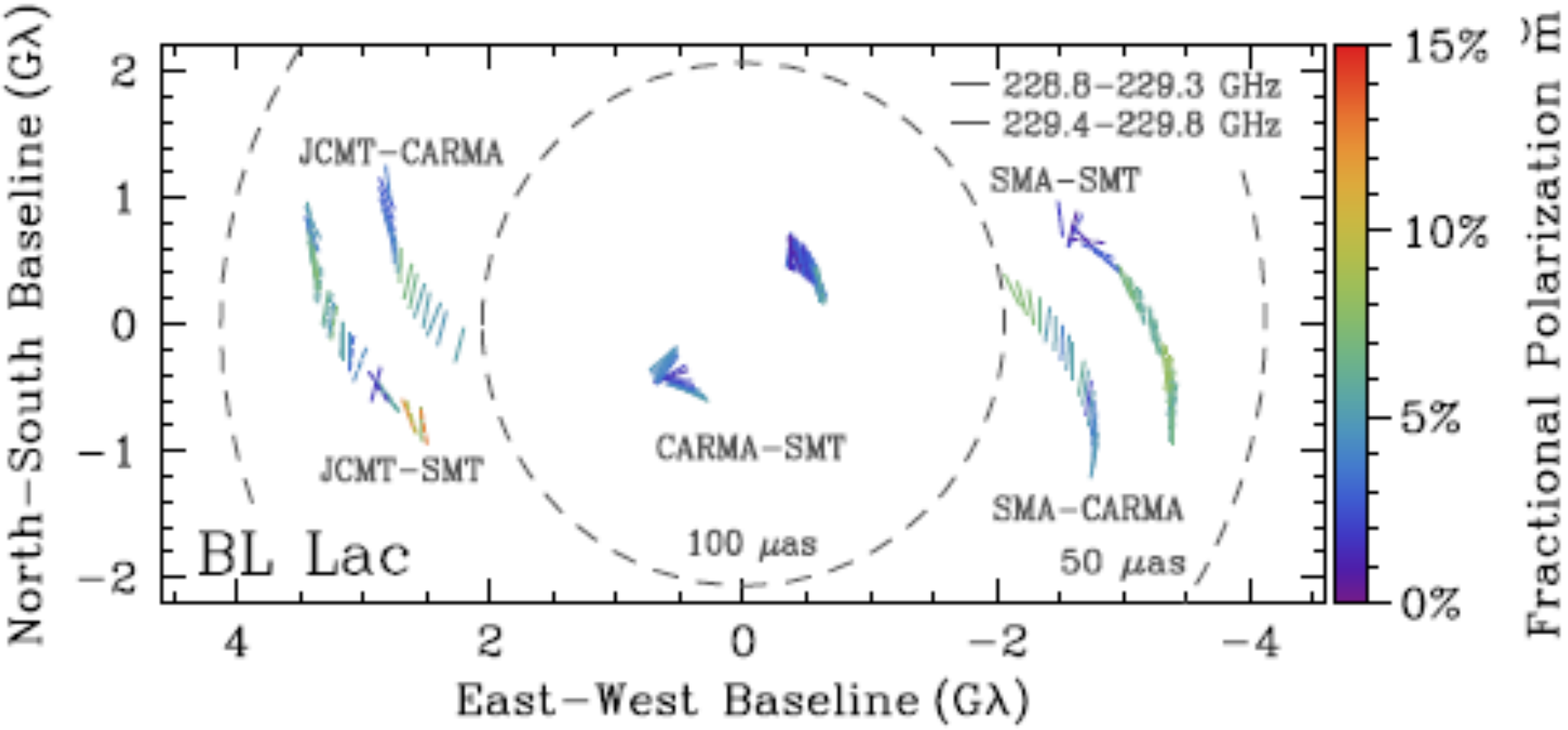

where $\breve{m}_k = \frac{\tilde{P}_k}{\tilde{I}_k}.$ is robust against atmospheric phase fluctuations

Sgr A* -- high fractional polarization on trans pacific baselines

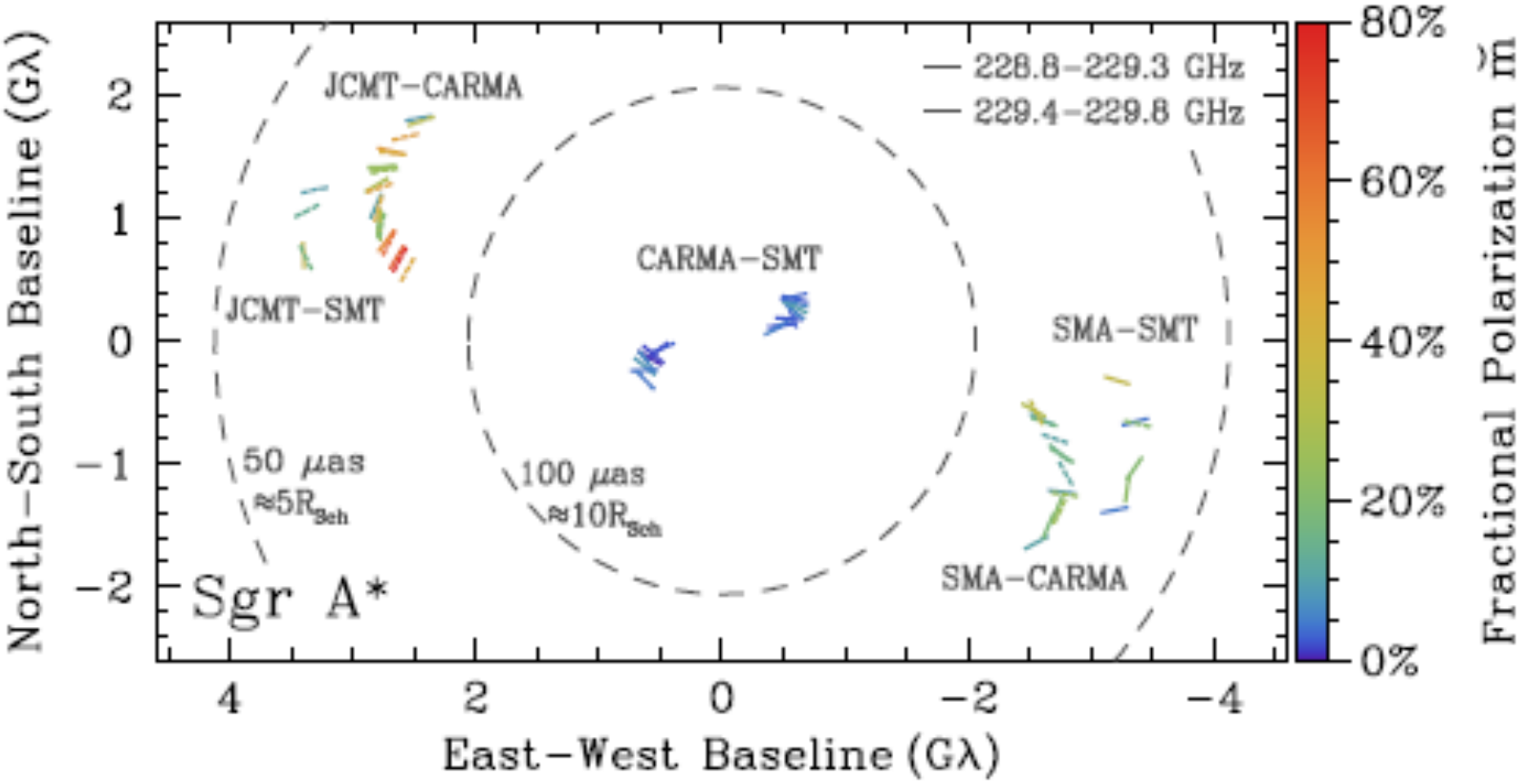

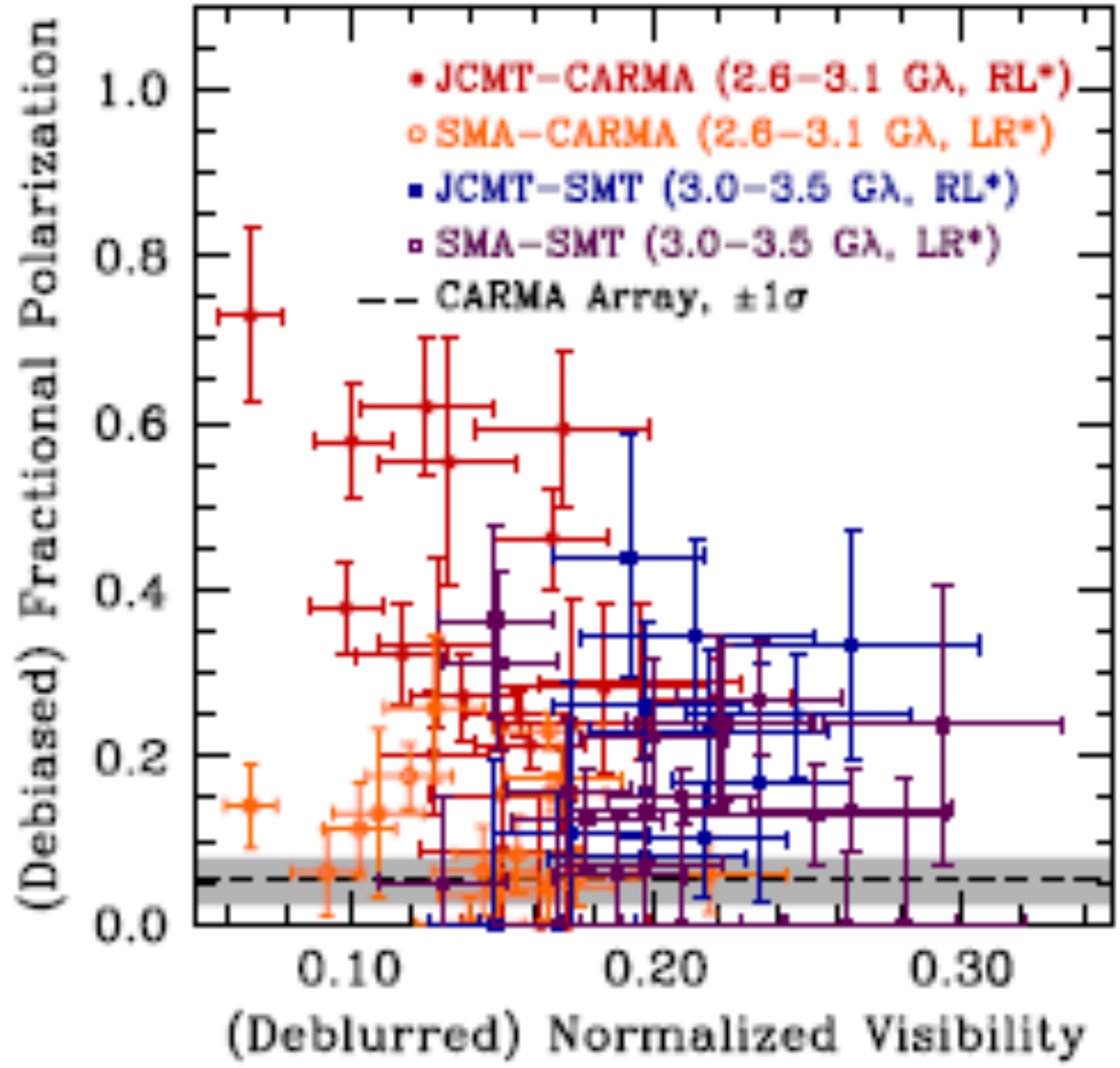
JCMT–CARMA (2.6–3.1 Gλ, RL*)
SMA–CARMA (2.6–3.1 Gλ, LR*)
JCMT–SMT (3.0–3.5 Gλ, RL*)
SMA–SMT (3.0–3.5 Gλ, LR*)
CARMA Array, ±1σ
(Debiased) Fractional Polarization
1.0
0.8
0.6
0.4
0.2
0.0
0.10
0.20
0.30
(Deblurred) Normalized Visibility

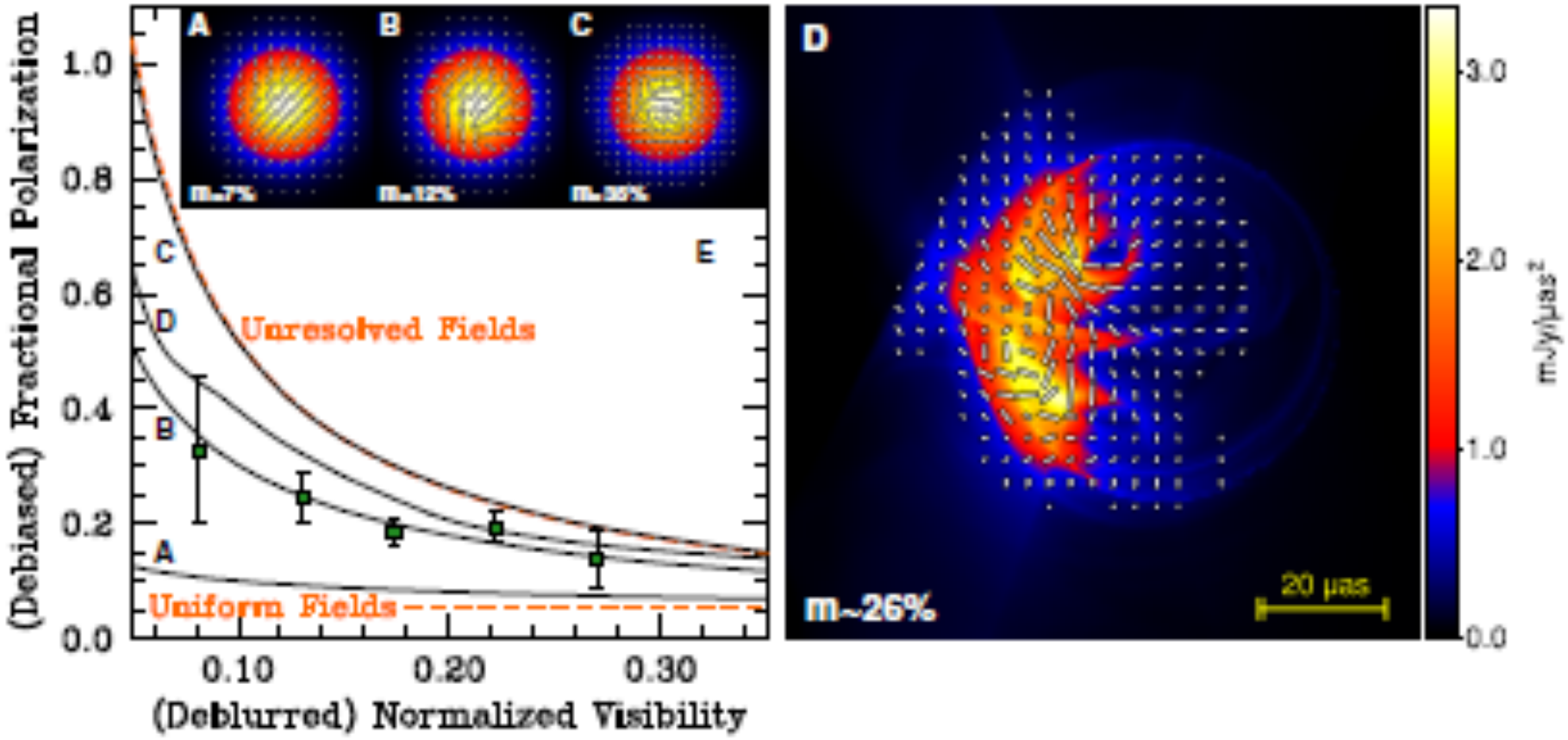

Image D is from Shcherbakov, Penna & McKinney (2012)

3. Polarized Maximum Entropy imaging

HIGH RESOLUTION LINEAR POLARIMETRIC IMAGING FOR THE EVENT HORIZON TELESCOPE

ANDREW A. CHAEL[1], MICHAEL D. JOHNSON[1], RAMESH NARAYAN[1], SHEPERD S. DOELEMAN[1,2], JOHN F. C. WARDLE[3], KATHERINE L. BOUMAN[4]

Draft version May 6, 2016

arXiv e-print (arXiv:1605.06156)

See also Coughlan & Gabuzda (2013) and Holdaway & Wardle (1990)

Total Intensity MEM:

Maximize an objective function $J = S(\mathbf{I}', \mathbf{B}) - \alpha \left(\chi^2(\mathbf{I}') - 1\right)$

Total Intensity MEM:

Maximize an objective function $J = S(\mathbf{I}', \mathbf{B}) - \alpha \left(\chi^2(\mathbf{I}') - 1\right)$

Entropy function:

$$S(\mathbf{I}', \mathbf{B}) = -\sum_{i=1}^{n^2} I'_i \log\left(\frac{I'_i}{B_i}\right)$$

Total Intensity MEM:

Maximize an objective function $J = S(\mathbf{I}', \mathbf{B}) - \alpha \left(\chi^2(\mathbf{I}') - 1\right)$

Entropy function:

$$S(\mathbf{I}', \mathbf{B}) = -\sum_{i=1}^{n^2} I'_i \log\left(\frac{I'_i}{B_i}\right)$$

Goodness of fit criterion:

$$\chi^2(\mathbf{I}') = \frac{1}{2N} \sum_{k=1}^{N} \frac{1}{\sigma_k^2} |\tilde{I}_k - \tilde{I}'_k|^2$$

Total Intensity MEM:

Maximize an objective function $J = S(\mathbf{I}', \mathbf{B}) - \alpha \left(\chi^2(\mathbf{I}') - 1\right)$

Entropy function:

$$S(\mathbf{I}', \mathbf{B}) = -\sum_{i=1}^{n^2} I'_i \log\left(\frac{I'_i}{B_i}\right)$$

Goodness of fit criterion:

$$\chi^2(\mathbf{I}') = \frac{1}{2N} \sum_{k=1}^{N} \frac{1}{\sigma_k^2} |\tilde{I}_k - \tilde{I}'_k|^2$$

Or using more robust VLBI measurables -- the bi-spectrum (closure phases):

$$\chi^2_B(\mathbf{I}') = \frac{1}{2N_B} \sum_{j=1}^{N_B} \frac{1}{\sigma^2_{B\,j}} |\tilde{I}_{B\,j} - \tilde{I}'_{B\,j}|^2$$

Polarization MEM:

Maximize an objective function: $J_m = S_m(\mathbf{P}') - \beta\left(\chi^2_m(\mathbf{I}', \mathbf{P}') - 1\right)$

Goodness of fit criterion: $\chi^2_m(\mathbf{I}', \mathbf{P}') = \frac{1}{2N}\sum_{k=1}^{N} \frac{1}{\sigma^2_{m\,k}} |\breve{m}_k - \breve{m}'_k|^2,$

where $\breve{m}_k = \tilde{P}_k/\tilde{I}_k$ is the complex fractional polarization of the kth u-v point

Entropy function:

$$S_m(\mathbf{P}') = -\sum_{i=1}^{n^2} I'_i \left[\frac{m_{\max} + m'_i}{2} \log\left(\frac{m_{\max} + m'_i}{2}\right) + \frac{m_{\max} - m'_i}{2} \log\left(\frac{m_{\max} - m'_i}{2}\right)\right]$$

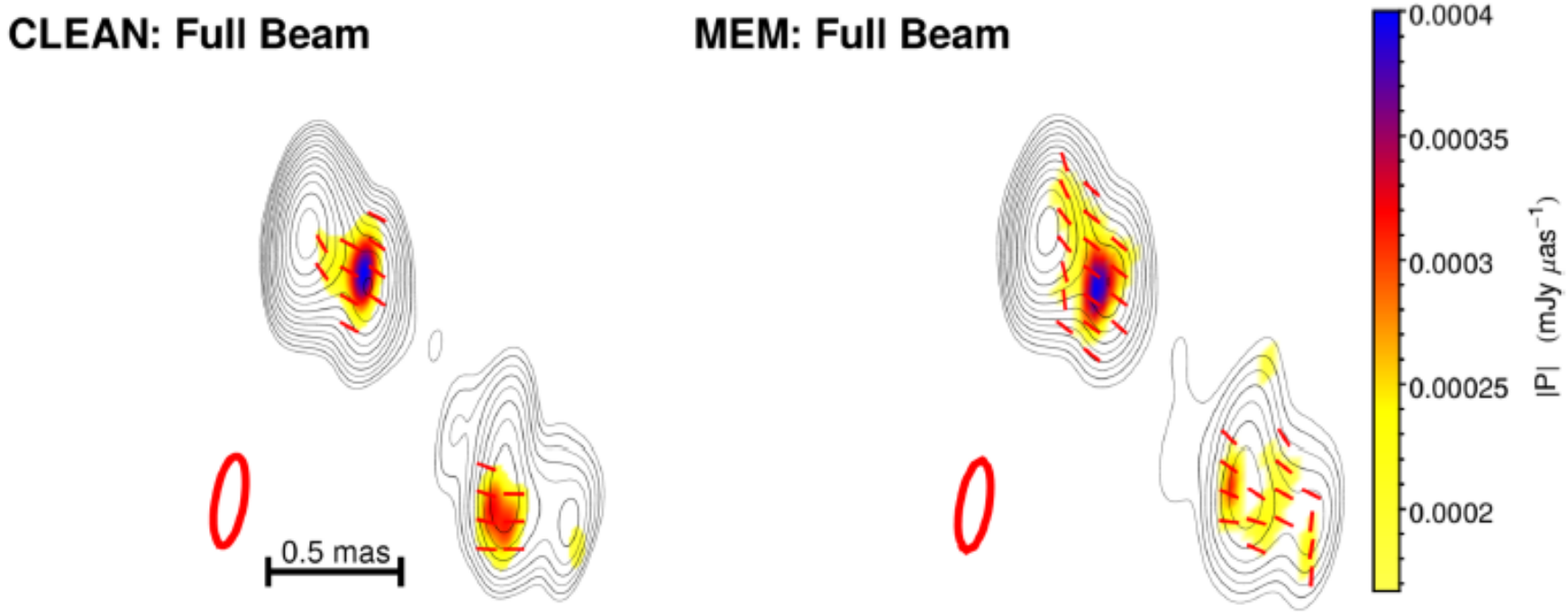

Figure 3. Reconstructions of 3-mm observations of the quasar 3C273 taken with the VLBA+GBT (Hada et al. 2016).

While the CLEAN reconstruction used a self-calibration loop to determine visibility phases on $\tilde{I}$, $\tilde{Q}$, and $\tilde{U}$, the MEM reconstruction directly used bispectrum and polarimetric ratio data. The MEM reconstruction used the Ponsonby-Nityananda-Narayan (PNN) entropy term.

Results on a model black hole image observed with a simulated EHT: Total Intensity

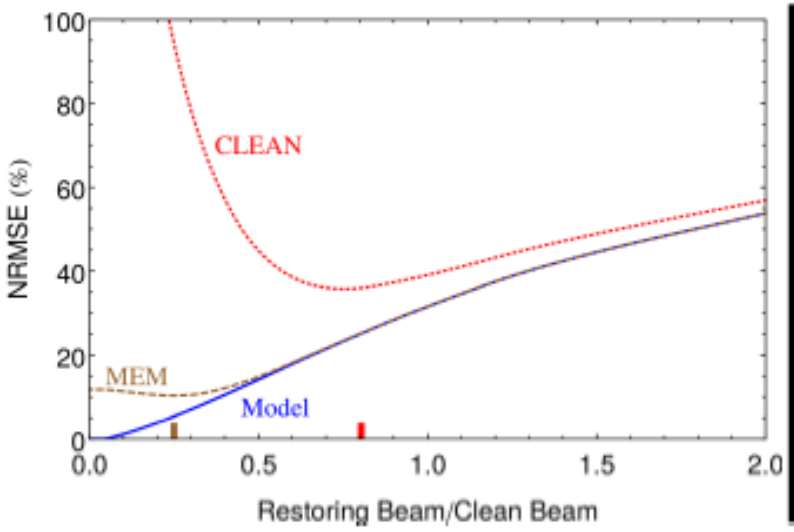

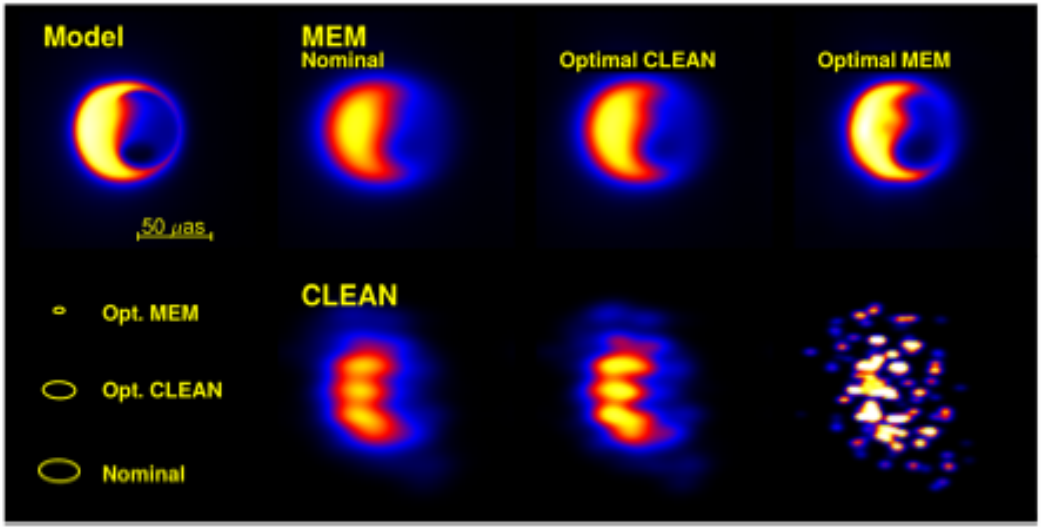

Results on a model black hole image observed with a simulated EHT: Polarization

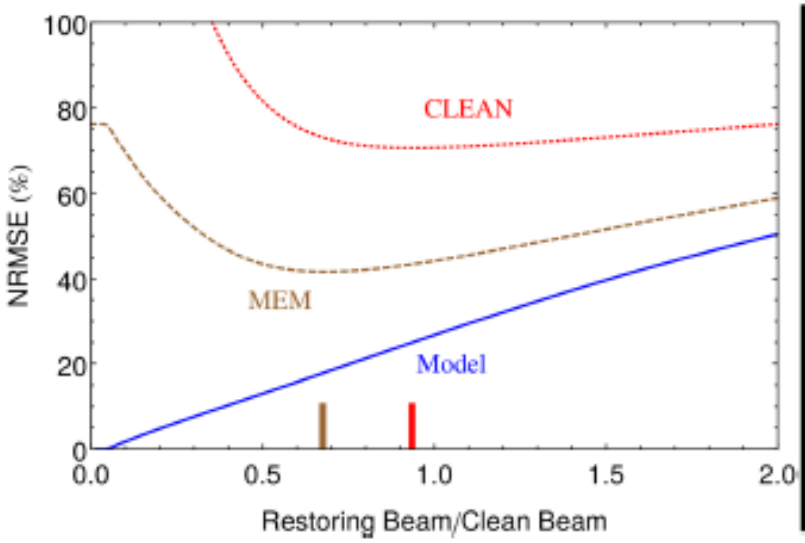

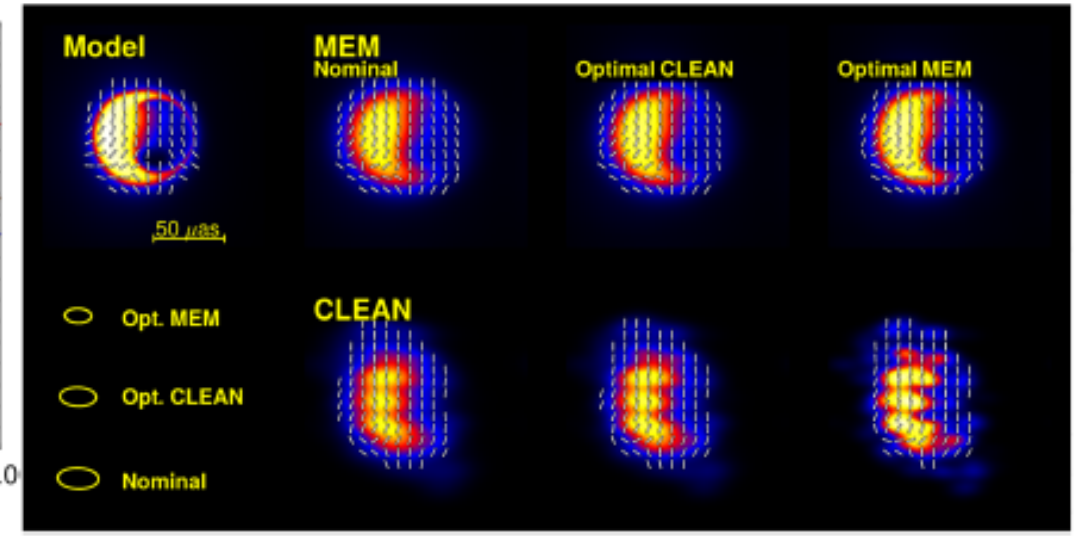

4. What the EHT might see

PROBING THE MAGNETIC FIELD STRUCTURE IN SGR A* ON BLACK HOLE HORIZON SCALES WITH POLARIZED RADIATIVE TRANSFER SIMULATIONS

ROMAN GOLD[1], JONATHAN C. MCKINNEY[1], MICHAEL D. JOHNSON[2], SHEPERD S. DOELEMAN[2,3]
[1]Department of Physics & Joint Space-Science Institute, University of Maryland, College Park, MD 20742
[2]Harvard-Smithsonian Center for Astrophysics, 60 Garden Street, Cambridge, MA 02138, USA and
[3]Massachusetts Institute of Technology, Haystack Observatory, Route 40, Westford, MA 01886, USA
Draft version January 22, 2016

arXiv e-print (arXiv:1601.05550)

1: 3-D GRHMD simulations of 2 MAD models, 2 SANE models

2: For each simulation, optimize 3 free parameters (inclination, accretion rate, and heating ratio between electrons and protons), by matching to the single dish spectra.

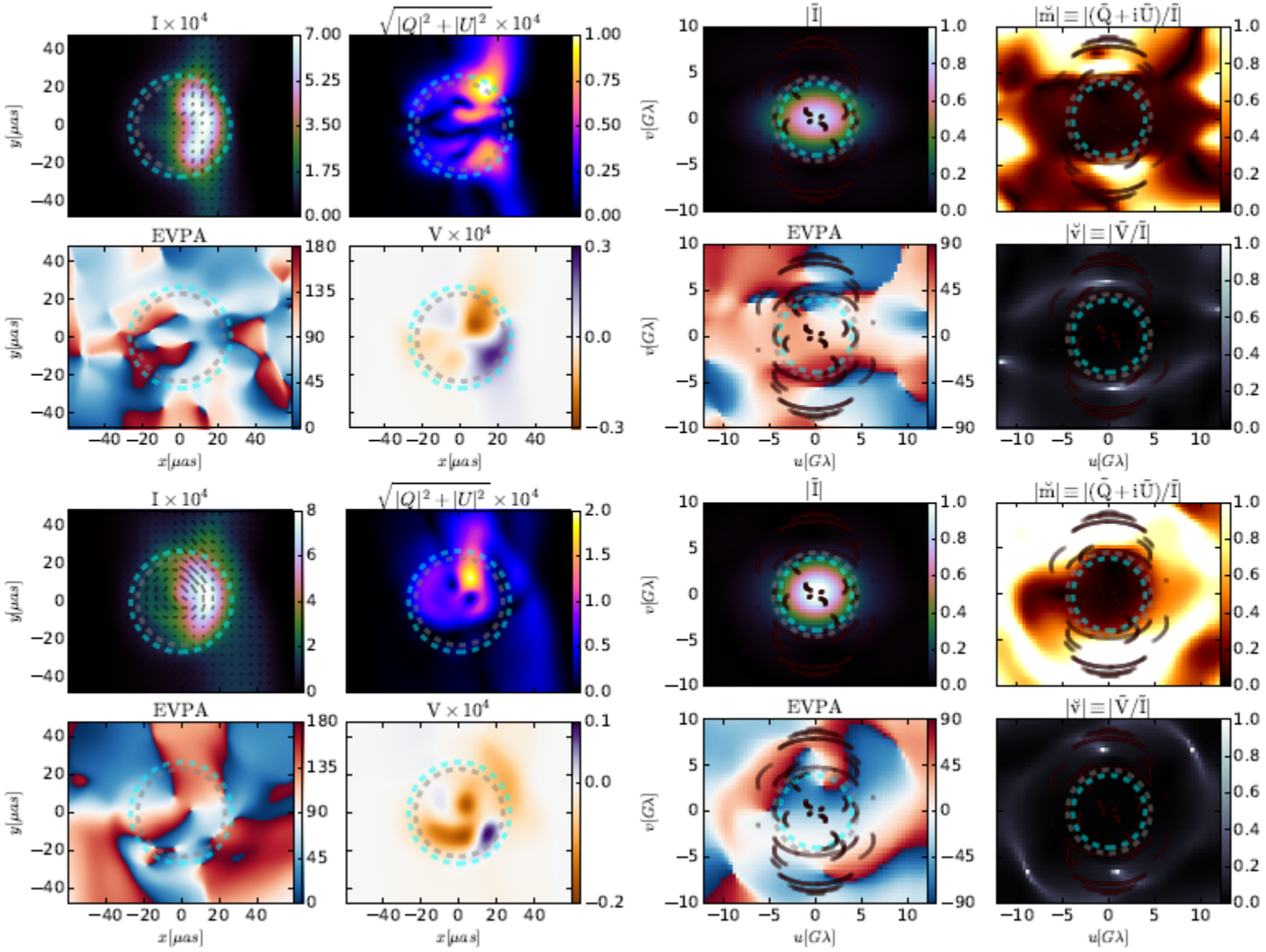

Upper two rows: MAD_thick-disk
Lower two rows: MAD_thick-jet

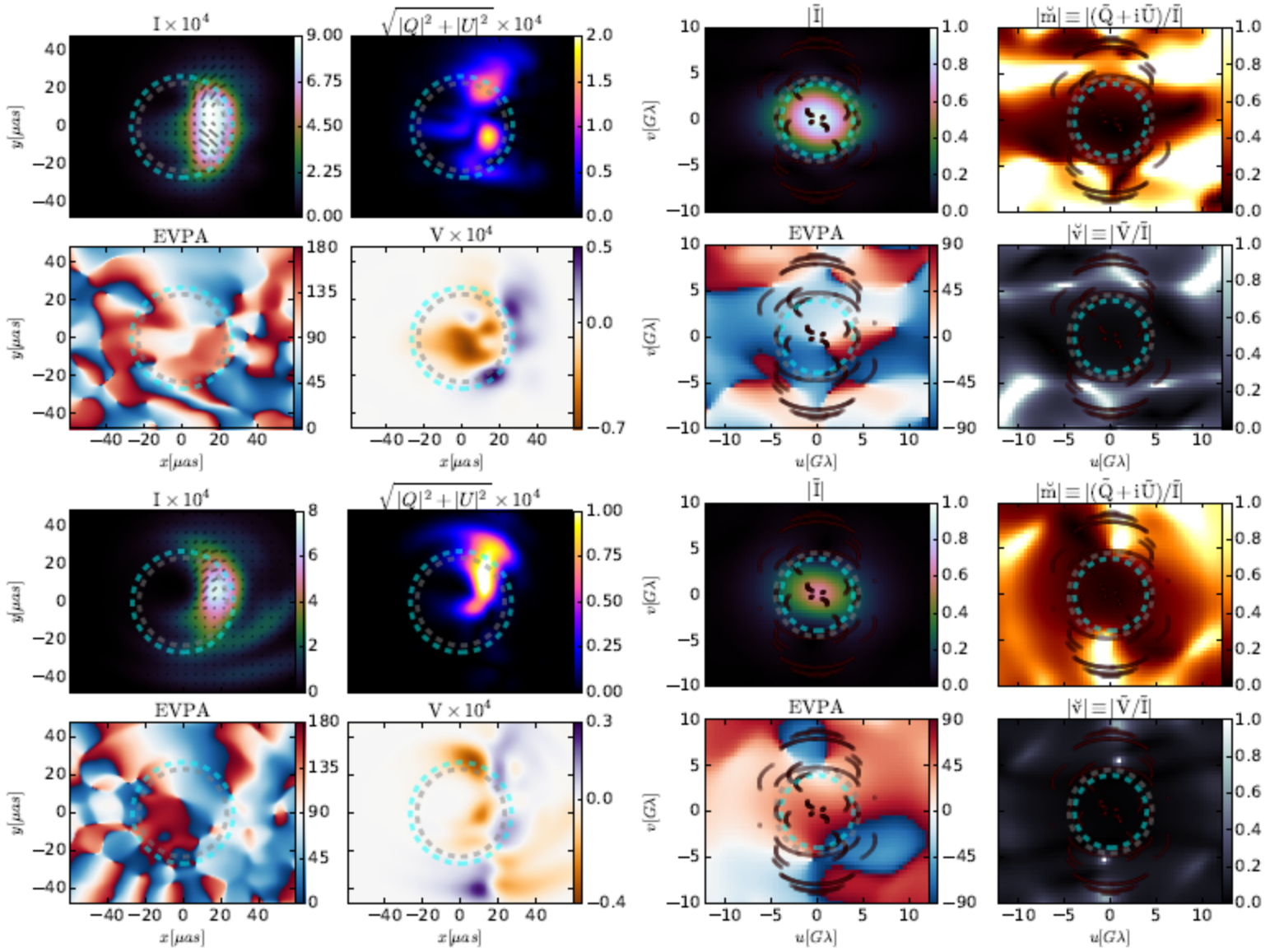

Upper two rows: SANE_quadrupole-disk
Lower two rows: SANE_dipole-jet

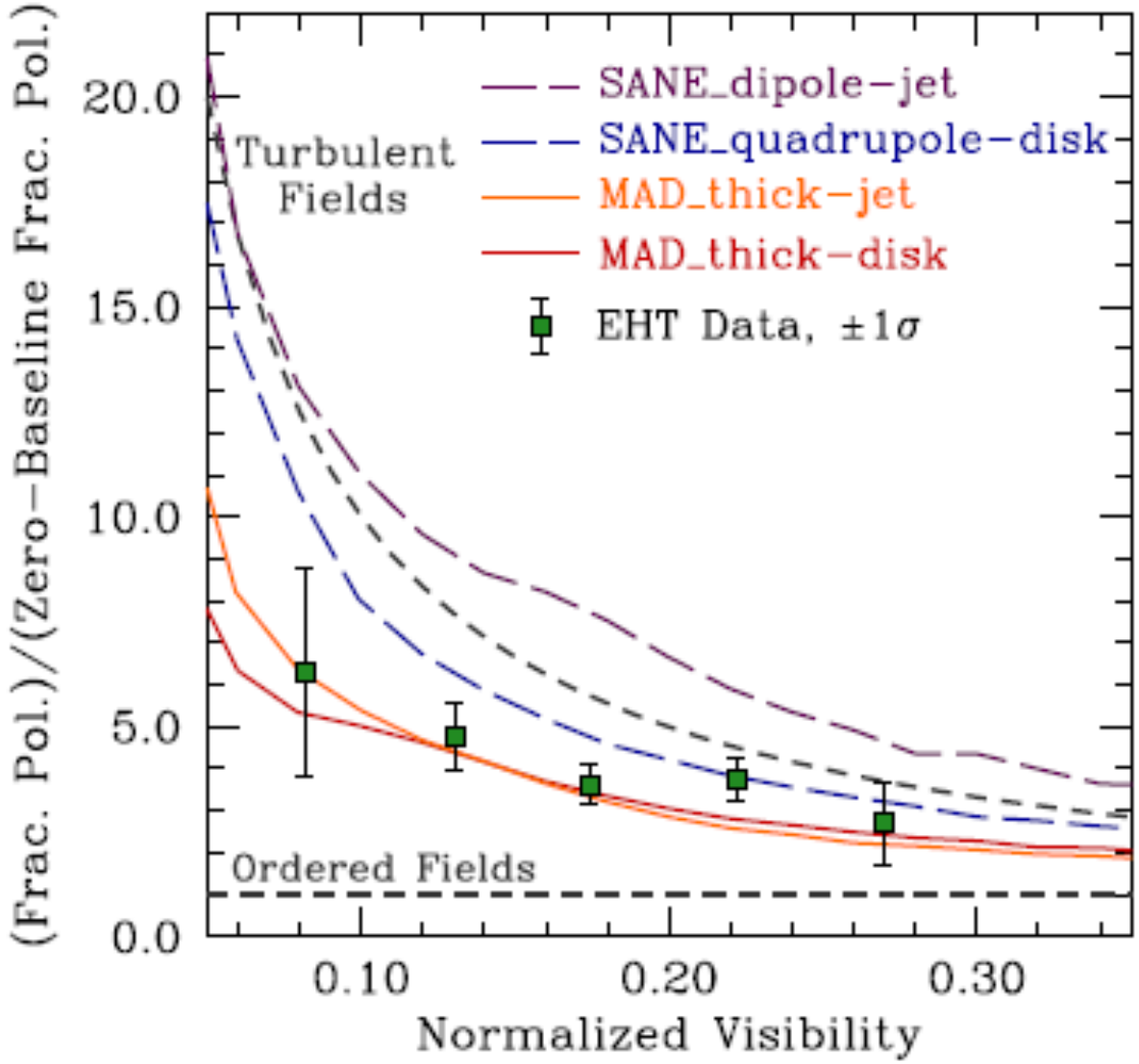

FIG. 8.— Fractional linear polarization $|\breve{m}|$ (as measured in the visibility plane) per unit zero baseline value vs. the normalized visibility $|\breve{I}/\breve{I}_0|$ for all models. Observational data from the EHT are shown as green squares.

MAD	SANE
marginally stable against the MRI	always disrupted by the MRI
makes jets	Makes weak jets with difficulty, or no jets at all

MAD	SANE
marginally stable against the MRI	always disrupted by the MRI
makes jets	Makes weak jets with difficulty, or no jets at all

CONJECTURE:

These are radio loud quasars (10%)	These are radio quiet quasars (90%)

5. Alan P. Marscher 1951 --


17
SEIDENBERG
44
VAUGHN


Reebok
CCM
TOEWS
19


“My Graduate Student Just Deleted All The Source Files”


“What do you mean, we forgot to observe any polarization calibrators?”


“What do you mean, Donald Trump might be the next president?”


DENTAL
DENTISTA
5ºB
RBOLARIO
ORIA NATURAL
MILLADERO
GR 3011 AX


HAPPY BIRTHDAY